

# Parametric study of die sinking EDM process on AISI H13 tool steel using statistical techniques

Bose, G.K.<sup>a,\*</sup>, Mahapatra, K.K.<sup>b</sup>

<sup>a</sup>Department of Mechanical Engineering, Haldia Institute of Technology, Haldia, India

<sup>b</sup>Technical Service, Central Institute of Plastic Engineering Technology, Bhubaneswar, India

## ABSTRACT

The correct optimization of process parameters is one of the more important aspects when taking into consideration the majority of manufacturing processes and particularly for processes relating to electrical discharge machining (EDM). It is capable of machining geometrically complex or hard material components that are precise and difficult-to-machine, such as heat-treated tool steels, composites, super alloys, ceramics, carbides, heat resistant steels etc. The presented study focused on the electric discharge machining (EDM) of AISI H 13, W.-Nr. 1.2344 Grade: Orvar Supreme for finding out the effect of machining parameters such as discharge gap current (GI), pulse on time (POT), pulse off time (POF) and spark gap (SG) on performance responses such as material removal rate (MRR), surface roughness ( $R_a$ ) and overcut (OC) using a square-shaped Cu tool with lateral flushing. A well-designed experimental scheme was used to reduce the total number of experiments. Parts of the experiment were conducted within the L27 orthogonal array based on the Taguchi method and significant process parameters were identified using analysis of variance (ANOVA). It was found that MRR is affected by gap current and  $R_a$  is affected by pulse on time. Moreover, the signal-to-noise ratios associated with the observed values in the experiments were determined by which factor was most affected by the responses of MRR,  $R_a$  and OC. These experimental data are investigated using response surface methodology (RSM) for the effects of four EDM parameters GI, POT, POF and SG on MRR,  $R_a$  and OC. Response surfaces and contour plots were considered for exploring the importance of the variables and their levels, so as to optimize the responses. Finally multi-response optimization was carried out by means of overlaid contour plots and desirability functions.

© 2014 PEI, University of Maribor. All rights reserved.

## ARTICLE INFO

### Keywords:

Die sinking EDM  
Multi response optimization  
Analysis of variance  
Response surface methodology

### \*Corresponding author:

gkbose@yahoo.com  
(Bose, G.K.)

### Article history:

Received 29 June 2014  
Revised 4 November 2014  
Accepted 10 November 2014

## 1. Introduction

Electro discharge machining (EDM) is an electro-thermal non-traditional machining process, where electrical energy is used to generate electrical spark and material removal mainly occurs due to thermal energy of the spark. The EDM process is employed widely for making tools, dies and other precision parts. It is capable of machining geometrically complex or hard material components, that are precise and difficult-to-machine such as heat treated tool steels, composites, super alloys, ceramics, carbides, heat resistant steels etc. In the Sinker EDM process, two metal parts submerged in an insulating liquid are connected to a source of current which is switched on and off automatically depending on the parameters set on the controller.

A brief literature review on EDM process is presented here. Selvakumar et al. [1] studied the experimental performance based on L-18 orthogonal array with pulse on time, pulse off time, peak current, wire tension, servo feed setting and corner angle as control factors. ANOVA was performed to find the significance of the factors considered. Kapoor et al. [2] investigated the effect of cryogenic treated brass wire electrode on surface roughness and material removal rate for WEDM. They described the influence of various machining parameters (including pulse width, time between two pulses, wire tension and wire feed) on surface roughness and material removal rate by using one variable at a time approach. Dvivedi et al. [3] investigated the EDM using Al 6063 SiCp metal matrix composite for surface quality. Aligiri [4] studied the real-time pulse discriminating system employed as the basic platform of micro-EDM control system for a more detailed interpretation of the state of micro-EDM process. Liu et al. [5] describes the use of adductive networks to monitor the electrical discharge machining (EDM) process. Ayesta et al. [6] studied parameters related to the discharge process (current, pulse time and servo voltage) on machining time and electrode wear in EDM process. Nipanikar [7] studied the cutting of D3 Steel material using EDM with a copper electrode by using Taguchi methodology. Salem et al. [8] predicted the surface roughness by experimental design methodology in EDM. Singh and Kalra [9] optimize the machining parameters of EDM on OHNS steel using the Taguchi method and ANOVA methods. Syed and Palaniyandi [10] has studied the performance of electrical discharge machining using Al powder suspended distilled water using Taguchi Design of Experiments. Kumar et al. [11] present an investigation on WEDM of pure titanium (grade-2) while determining surface roughness using multi response optimization. Kohli et al. [12] studied the machining of medium carbon steel (AISI 1040) using die sinking EDM with input parameters like discharge current ( $I_p$ ), pulse on time ( $T_{on}$ ), pulse off time ( $T_{off}$ ). Mohanty et al. [13] presented a thermal-structural model to analyze the process parameters and their effect on responses like MRR, tool wear rate and residual stresses using EDM process. Arikatla et al. [14] studied the optimization of EDM using design of experiment. Baseri et al. [15] investigated the effects of the flushing types on rotary electro discharge machining performance using alloy steel of X210Cr12.

The objective of the work is to study the characteristic features of the EDM process as reflected through Taguchi design based experimental studies with various process parametric combinations like gap current (GI), pulse on time (POT), pulse off time (POF), and spark gap (SG) on material removal rate (MRR), surface roughness ( $R_a$ ), and overcut (OC). The significant process parameters are identified using analysis of variance (ANOVA). These experimental data are further investigated using response surface methodology (RSM). The present paper is aimed at fulfillment of two basic but conflicting objectives concurrently higher material removal rate (MRR) and lower surface roughness ( $R_a$ ) by employing a single set of optimal or near optimal process variables following response surface methodology (RSM). Response surfaces and contour plots are studied to investigate the prominence of the variables and their levels so as to optimize the responses. Finally multi-response optimization is carried out using overlaid contour plots and desirability functions.

## 2. Planning for experimentation

In the present research work electric discharge machine (ACTSPARK SP1, China) die-sinking type with servo-head (constant gap) and positive polarity for electrode is used for experimentation. Commercial grade EDM-30 oil (specific gravity of 0.80 at 25 °C, viscosity of  $3.11 \times 10^{-6} \text{ m}^2\text{s}^{-1}$  at 38 °C) was used as dielectric fluid. With external lateral flushing using a square-shaped Cu tool (12 mm × 12 mm) having a pressure 0.2 kgf/cm<sup>2</sup> is used. Experiments were conducted with positive polarity of electrode. AISI H-13 Tool steel work piece material is selected for the experiment. The pulsed discharge current was applied in various steps in positive mode. The EDM set-up consists of dielectric reservoir, pump and circulation system, power generator and control unit, working tank with work holding device, X-Y table accommodating the working table, tool holder and the servo system to feed the tool part. The servo control unit is provided to maintain the pre-determined gap. It senses the gap voltage and compares it with the present value and the different in voltage is then used to control the movement of servo motor to adjust the gap. The

MRR is expressed as the ratio of the volume of the work piece material removed during machining the cavity to the machining time. Surface roughness of the cavity surface is expressed as  $R_a$  ( $\mu\text{m}$ ) and measured using stylus type profilometer named Talysurf (Taylor's Hobson Surtronic 3+). Overcut is expressed as half the difference of area of the cavity produced to the tool frontal area. Area of cavity and frontal area of electrode can be calculated by measuring the respective length and width using Toolmaker's microscope.

When performing an experiment, varying the levels of the factors simultaneously rather than one at a time is efficient in terms of time and cost, and also allows for the study of interactions between the factors. Based on past research works and preliminary investigation, four parameters were chosen as input. Initially L9 orthogonal array is employed for the experimentation. The input parameters were varied with three levels in nine experimental run. There are other factors which may affect the measured performance like duty cycle, flushing pressure, lift time etc., however, were kept constant during experimentation. Table 1 exhibits the different levels of control parameters during machining process.

**Table 1** Parametric settings and responses for experimental run

Expt. No.	Control parameters				Responses		
	POT ( $\mu\text{s}$ )	POF ( $\mu\text{s}$ )	GI (A)	SG (mm)	MRR ( $\text{mm}^3/\text{s}$ )	$R_a$ ( $\mu\text{m}$ )	OC ( $\text{mm}^2$ )
1	16	12	7	0.16	0.0346	9.6	4.237
2	16	16	9	0.18	0.0933	10.733	2.358
3	16	20	11	0.2	0.1441	11.133	3.556
4	20	12	9	0.2	0.1581	7.6	4.469
5	20	16	11	0.16	0.2064	9.4	4.349
6	20	20	7	0.18	0.0133	6.6	3.376
7	24	12	11	0.18	0.1267	7.93	3.241
8	24	16	7	0.2	0.0085	3.467	3.124
9	24	20	9	0.16	0.0943	9.2	4.876

### 3. Results analysis using ANOVA

ANOVA is a functional method for estimating error variance and determining the relative importance of various process variables [16]. The experimental outcomes are explored to study the role of different process variables on various responses by using S/N ratio and ANOVA. The result analysis is carried out by statistical software MINITAB, version 13.

S/N ratio determines the contribution of different process variables on various responses. The goal is to find out an optimal combination of control factor settings that achieve robustness against (insensitivity to) noise factors. S/N ratio analysis for MRR ( $\text{mm}^3/\text{min}$ ) is carried out on the basis of larger is the better and the corresponding S/N ratio is expressed as follows:

$$n_1 = -10\log_{10} \left( \frac{1}{n} \sum_{i=1}^n \frac{1}{MRR^2} \right) \quad (1)$$

S/N ratio analysis for  $R_a$  is modeled on the basis of smaller is the better and corresponding equation is

$$n_2 = -10\log_{10} \left( \frac{1}{n} \sum_{i=1}^n R_a^2 \right) \quad (2)$$

S/N ratio analysis for OC is modeled on the basis of smaller is the better and corresponding equation is

$$n_3 = -10\log_{10} \left( \frac{1}{n} \sum_{i=1}^n OC^2 \right) \quad (3)$$

The S/N plot for MRR,  $R_a$  and overcut are shown in Fig. 1.

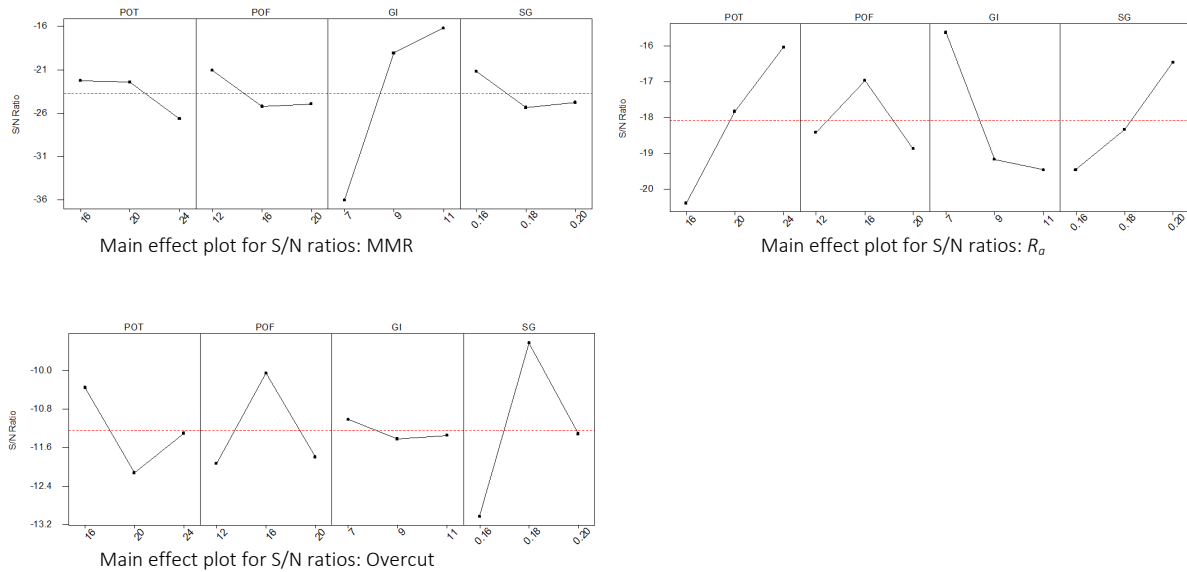


Fig. 1 S/N ratio plot for MRR,  $R_a$ , and overcut

It is observed from the S/N ratio graph that the MRR attains its peak with the parametric combination of POT (16  $\mu$ s), POF (12  $\mu$ s), GI (11 A), SG (0.16 mm). For smaller is better for  $R_a$  is obtained at POT (24  $\mu$ s), POF (16  $\mu$ s), GI (7 A), SG (0.20 mm). Similarly for smaller is better for OC is obtained at POT (16  $\mu$ s), POF (16  $\mu$ s), GI (7 A), SG (0.18 mm).

ANOVA results as exhibited from F-values and percentage contribution of the process variables states that the F-values of gap current assume value 22.337 with a yield of 82.28 % in case of MRR. This implies that the variable have significant effects on MRR. Whereas in case of  $R_a$ , pulse on time (POT) alone is the major contributor having F-value of healthy 5.34 and having percentage contribution of 47.24 %, which is widely followed by gap current having F-value of approximately 4. Finally in case of overcut the spark gap (SG) alone is the major contributor having F-value of healthy 4.0 with percentage contribution of 65.60 %. Other factors here remain insignificant.

#### 4. Results analysis using response surface methodology (RSM)

The response surface (output) can be related with the number of controllable variables  $x_1, x_2, \dots, x_k$  as

$$y = f(x_1, x_2, \dots, x_k) + \varepsilon \tag{4}$$

A second order model is used to establish input-output relationship efficiently that takes the generic form

$$y = \beta_0 + \sum_{i=1}^k \beta_i x_i + \sum_{i=1}^k \beta_{ii} x_i^2 + \sum_{i=1}^k \beta_{ij} x_i x_j + \varepsilon \tag{5}$$

The predicted response for the model is

$$\hat{y} = \hat{\beta}_0 + \sum_{i=1}^k \hat{\beta}_i x_i + \sum_{i=1}^k \hat{\beta}_{ii} x_i^2 + \sum_{i=1}^k \hat{\beta}_{ij} x_i x_j \tag{6}$$

In the present work, Box-Behenken design is followed which is based on  $2^k$  ( $k = 4$ ) factorials with incomplete designs and found to be very efficient [17]. The process variables combinations and the corresponding responses are presented in Table 2.

**Table 2** Combination of factors and responses for RSM

Expt. No.	POT ( $\mu\text{s}$ )	POF ( $\mu\text{s}$ )	GI (A)	SG (mm)	MRR ( $\text{mm}^3/\text{s}$ )	$R_a$ ( $\mu\text{m}$ )	Overcut ( $\text{mm}^2$ )
1	20	12	11	0.18	1.2578	9.467	2.529
2	24	20	9	0.18	0.1572	2.067	3.498
3	24	16	11	0.18	0.832	7.6	5.3177
4	20	20	7	0.18	0.0956	2.267	2.7668
5	16	16	11	0.18	2.0271	9.067	2.892
6	20	16	7	0.16	0.07652	5.467	3.739
7	16	20	9	0.18	0.4193	7.733	4.9574
8	20	20	11	0.18	1.1941	11.367	5.6864
9	20	16	11	0.2	1.6	12.667	5.2014
10	24	16	9	0.16	0.0969	3.067	3.4982
11	20	16	9	0.18	0.0479	11.467	3.2556
12	16	16	7	0.18	0.0367	8.133	2.166
13	20	12	9	0.2	0.1581	7.6	4.4686
14	16	16	9	0.16	0.17158	8.867	3.376
15	20	16	9	0.18	0.1383	8.867	4.5915
16	20	16	11	0.16	0.2064	9.4	4.3488
17	20	20	9	0.16	0.08905	9.467	2.2852
18	20	16	9	0.18	0.095	8.667	3.2536
19	20	20	9	0.2	0.0771	9.333	5.4462
20	20	12	9	0.16	0.0773	9.333	1.4424
21	20	16	7	0.2	0.00877	8	1.6827
22	16	16	9	0.2	0.0892	11.6	2.8896
23	16	12	9	0.18	0.17357	9.867	2.0444
24	24	12	9	0.18	0.0324	3.933	1.9248
25	24	16	9	0.2	0.116	11.733	3.6187
26	24	16	7	0.18	0.00636	5.333	3.498
27	20	12	7	0.18	0.01333	6.6	3.376

#### 4.1 Analysis of test results for material removal rate (MRR)

The estimated regression surface equation for MRR is:

$$\text{MRR} = -2.59 - 0.0349 \text{ POT} + 0.0032 \text{ POF} + 0.287 \text{ GI} + 5.55 \text{ SG} \quad (7)$$

The details of the regression analysis result are presented in Table 3. R-square as well as R-square (adjusted) assumes a value of 90.9 % and 80.2 %, respectively, that implies the model is poised to explain 90.9 % variability with process variable POT, POF, GI and SG. From the T-values of the process variables it can be concluded that GI is the most significant process variables followed by SG, POF and POT.

**Table 3** Estimated regression coefficients for material removal rate (MRR)

Term	Coef.	SE Coef.	T	P
Constant	0.0937	0.13894	0.675	0.513
POT	-0.1397	0.06947	-2.011	0.067
POF	0.0129	0.06947	0.186	0.855
GI	0.5733	0.06947	8.253	0.000
SG	0.1110	0.06947	1.597	0.136
POT*POT	0.0974	0.10421	0.935	0.368
POF*POF	0.0457	0.10421	0.439	0.669
GI*GI	0.4970	0.10421	4.769	0.000
SG*SG	-0.0765	0.10421	-0.734	0.477
POT*POF	-0.0302	0.12033	-0.251	0.806
POT*GI	-0.2912	0.12033	-2.420	0.032
POT*SG	0.0254	0.12033	0.211	0.837
POF*GI	0.0046	0.12033	0.039	0.970
POF*SG	-0.0232	0.12033	-0.193	0.850
GI*SG	0.3653	0.12033	3.036	0.010

Notes: S = 0.2407 R-Sq = 90.9 % R-Sq(adj) = 80.2 %

The response surface plots of MRR with respect to GI, SG, POT and POF are shown in Fig. 2. It is observed that high levels of the two variables out of four yield maximum responses. The GI and SG have the significant effect on MRR. Since the response is proportional to the variables, there can not have any stationary point as evident from the surface plots. Further, the effect of GI is more pronounced than other three parameters. It is observed that high levels of the two variables out of four yield maximum responses. The GI and SG have the significant effect on MRR. Since the response is proportional to the variables, there can not have any stationary point as evident from the surface plots. Further, the effect of GI is more pronounced than other three parameters.

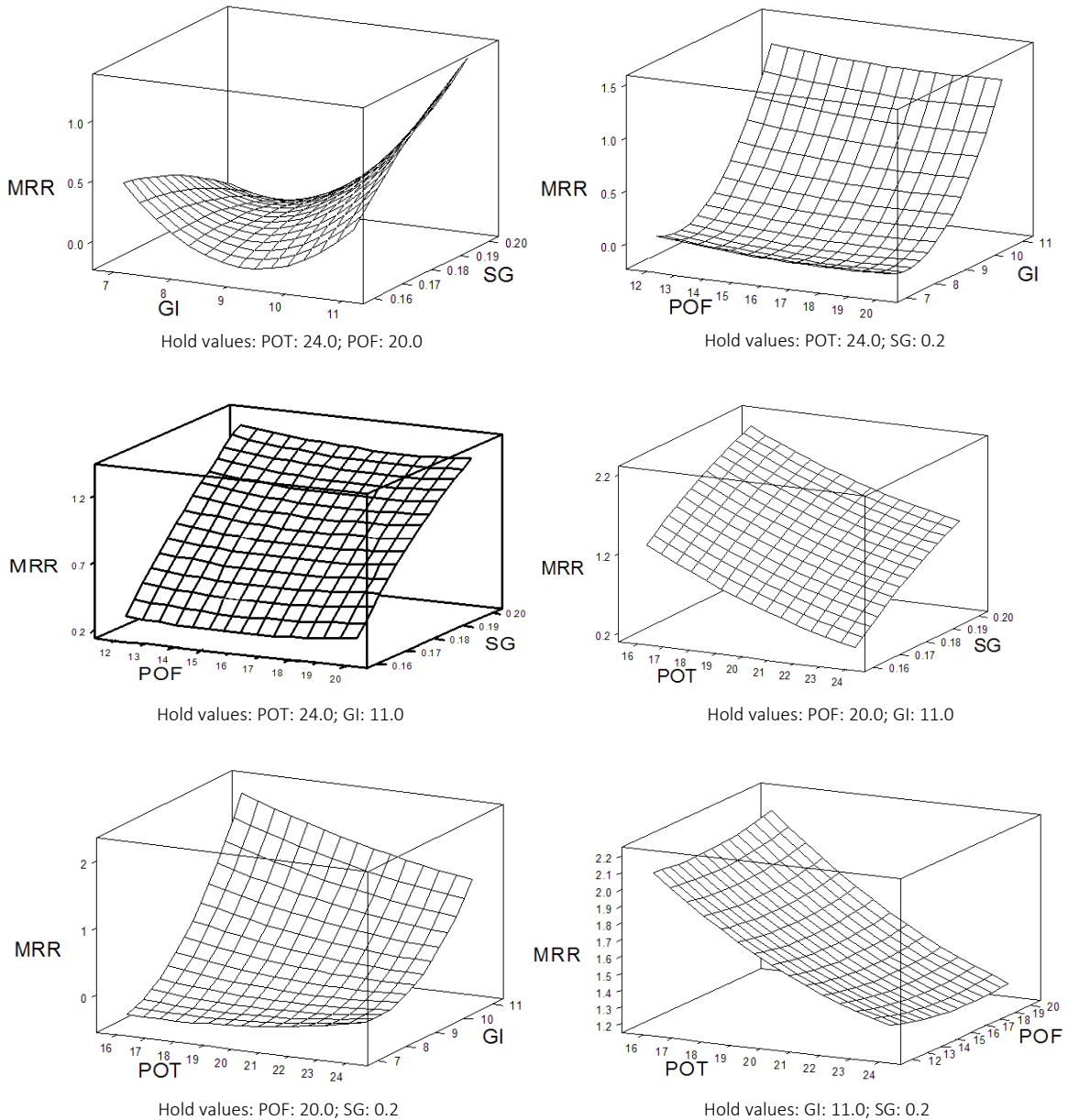


Fig. 2 Wire frame surface plot for MRR

4.2 Analysis of test results for surface roughness ( $R_a$ )

The estimated regression surface equation for  $R_a$  is:

$$RA = -4.70 - 0.449 POT + 0.085 POF + 0.990 GI + 63.9 SG \tag{8}$$

The particulars of the regression analysis outcome are presented in Table 4. R-square as well as R-square (adjusted) furnishes a value of 71.4 % and 38.0 %, respectively, that implies the

model is balanced to explain 71 % variability with process variable POT, POF, GI and SG. From the T values of the process variables, it can be concluded that GI is the most significant process variables followed by SG, POF and POT.

The response surface plots of  $R_a$  with respect to GI, SG, POT and POF are shown in Fig. 3. It is seen that high levels of the two variables out of four capitulate utmost responses. The GI and SG have the considerable effect on  $R_a$ . Since the response is proportional to the variables, there can not have any stationary point as evident from the surface plots. Further, the effect of GI is more pronounced than other three parameters.

**Table 4** Estimated regression coefficients for surface roughness ( $R_a$ )

Term	Coef.	SE Coef.	T	P
Constant	9.667	1.3010	7.430	0.000
POT	-1.795	0.6505	-2.759	0.017
POF	0.342	0.6505	0.525	0.609
GI	1.981	0.6505	3.045	0.010
SG	1.278	0.6505	1.964	0.073
POT*POT	-1.624	0.9758	-1.664	0.122
POF*POF	-1.620	0.9758	-1.660	0.123
GI*GI	-0.828	0.9758	-0.848	0.413
SG*SG	0.568	0.9758	0.582	0.571
POT*POF	0.067	1.1267	0.059	0.954
POT*GI	0.333	1.1267	0.296	0.772
POT*SG	1.483	1.1267	1.316	0.213
POF*GI	-0.608	1.1267	-0.540	0.599
POF*SG	0.400	1.1267	0.355	0.729
GI*SG	0.184	1.1267	0.163	0.873

Notes: S = 2.253 R-Sq = 71.4 % R-Sq(adj) = 38.0 %

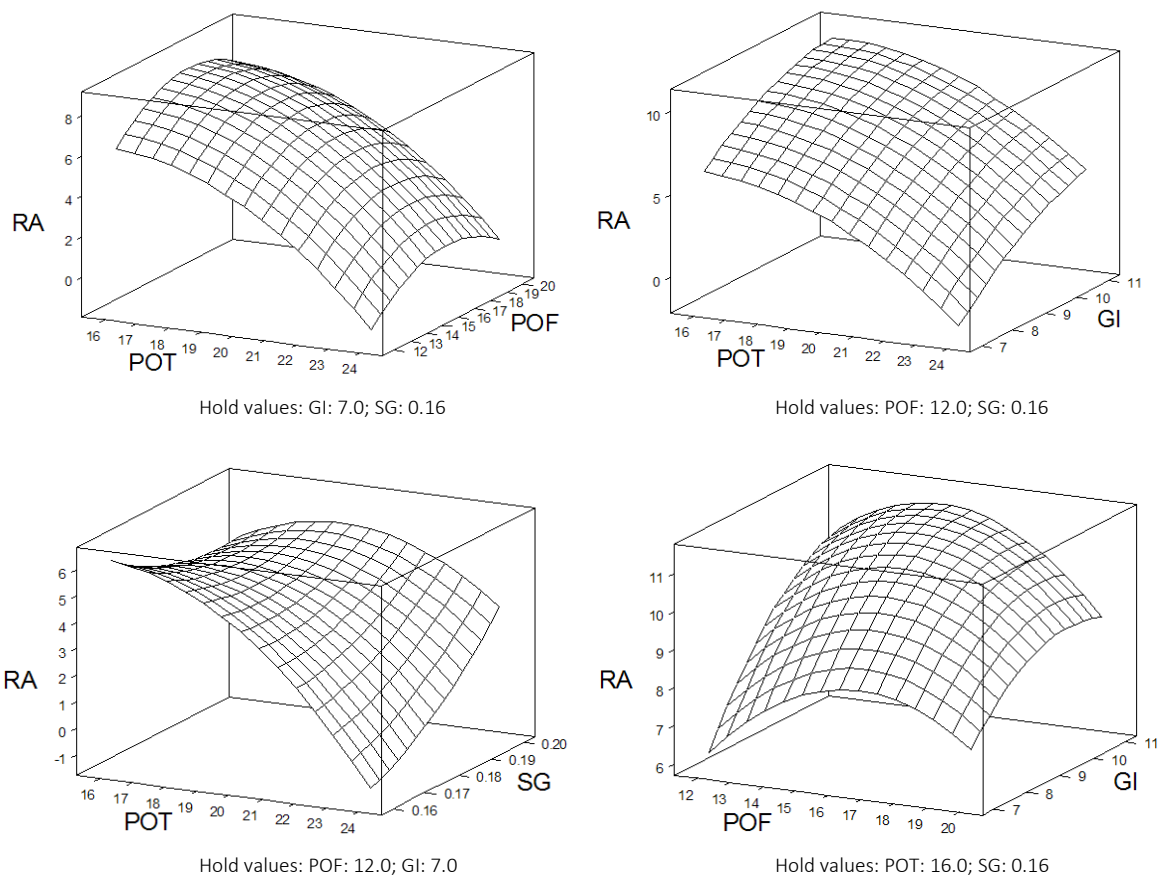


**Fig. 3** Wire frame surface plot for  $R_a$

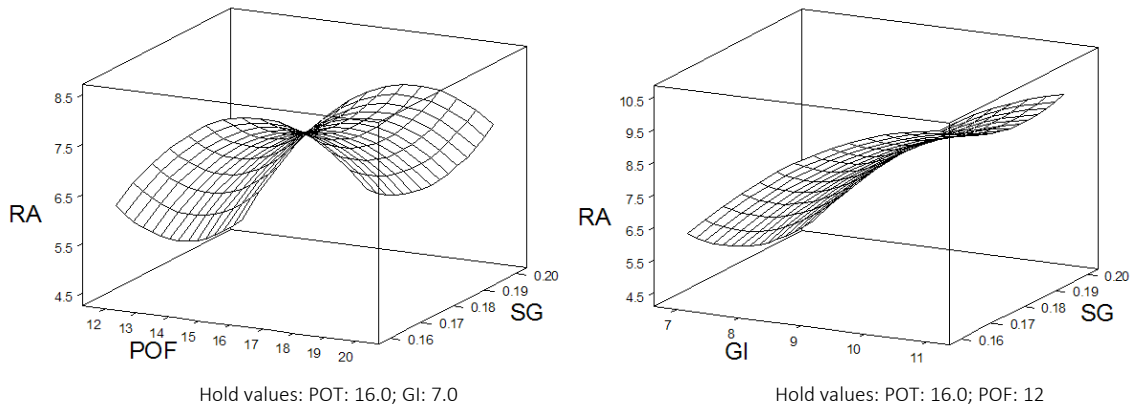


Fig. 3 Wire frame surface plot for  $R_a$  (continuation)

4.3 Analysis of test results for overcut (OC)

The estimated regression surface equation for overcut (OC) is:

$$OC = -4.70 - 0.449 POT + 0.085 POF + 0.990 GI + 63.9 SG \tag{9}$$

The particulars of the regression analysis are presented in Table 5. R-square furnishes a value of 61.4 % that implies the model is balanced to explain 61 % variability with process variable POT, POF, GI and SG. From the T values of the process variables, it can be concluded that POF is the most significant process variables followed by GI, SG and POT.

Table 5 Estimated regression coefficients for overcut (OC)

Term	Coef.	SE Coef.	T	P
Constant	3.7002	0.6344	5.833	0.000
POT	0.2525	0.3172	0.796	0.441
POF	0.8394	0.3172	2.646	0.021
GI	0.7289	0.3172	2.298	0.040
SG	0.3848	0.3172	1.213	0.248
POT*POT	-0.3339	0.4758	-0.702	0.496
POF*POF	-0.2409	0.4758	-0.506	0.622
GI*GI	0.1065	0.4758	0.224	0.827
SG*SG	-0.0444	0.4758	-0.093	0.927
POT*POF	-0.3350	0.5494	-0.610	0.553
POT*GI	0.2734	0.5494	0.498	0.628
POT*SG	0.1517	0.5494	0.276	0.787
POF*GI	0.6371	0.5494	1.160	0.269
POF*SG	0.0337	0.5494	0.061	0.952
GI*SG	0.7272	0.5494	1.324	0.210

Notes: S = 1.099 R-Sq = 61.4 % R-Sq(adj) = 16.4 %

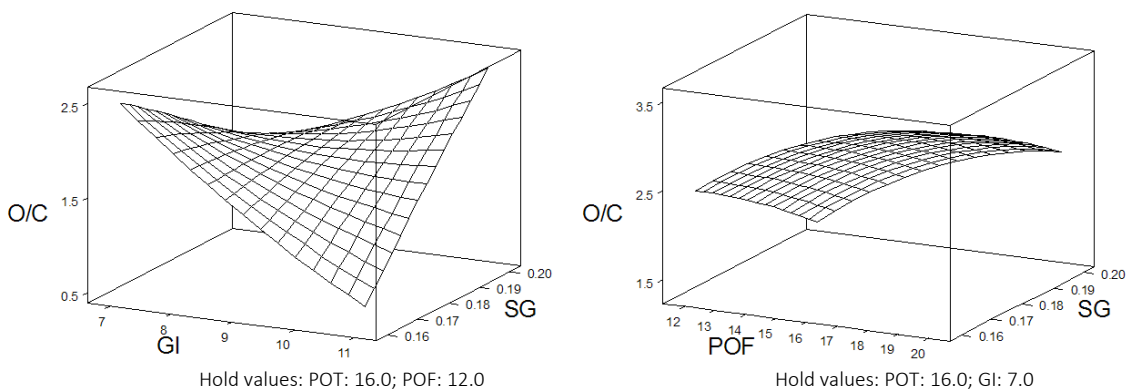
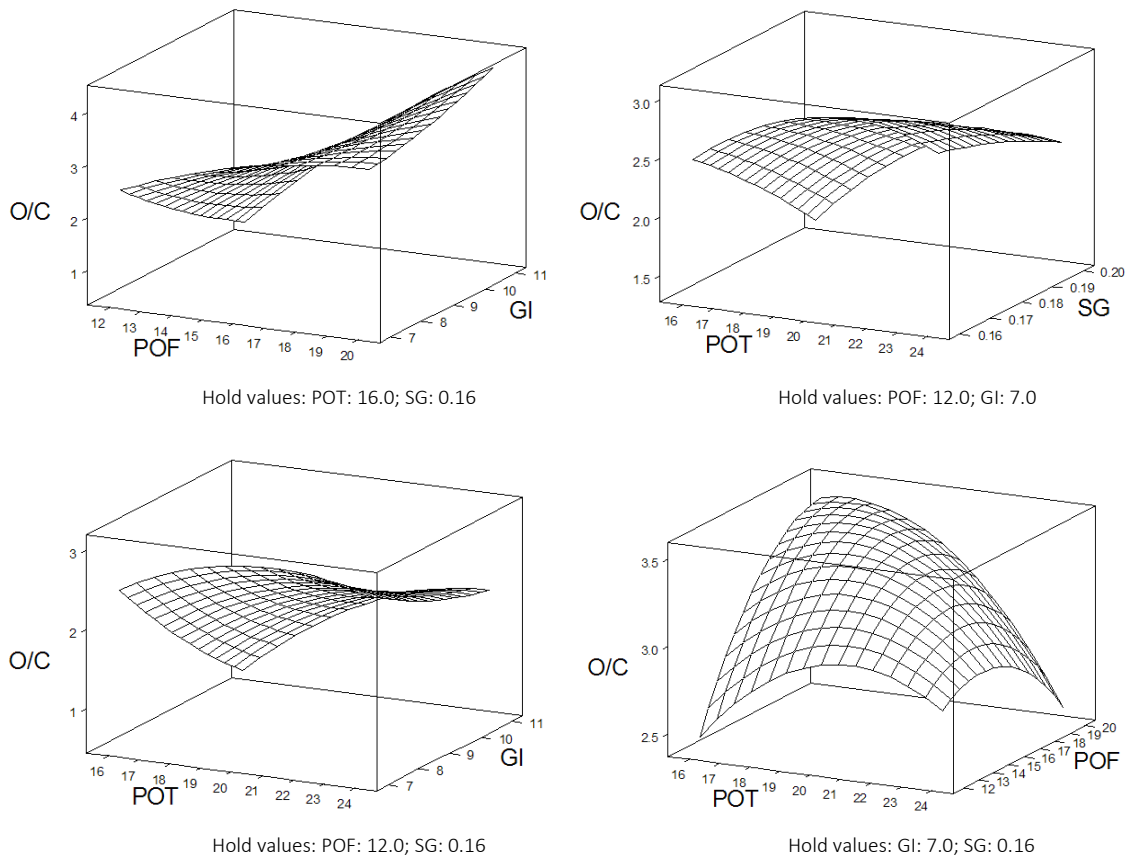


Fig. 4 Wire frame surface plot for overcut





**Fig. 4** Wire frame surface plot for overcut (continuation)

The response surface plots of  $R_a$  with respect to GI, SG, POT and POF are shown in Fig. 4. It is seen that high levels of the two variables out of four capitate utmost responses. Since the response is proportional to the variables, there can not have any stationary point as evident from the surface plots. It is observed that the two variables out of four yield maximum responses. It clears that the POF and GI are the significant parameter for O/C.

## 5. Multi response optimization

### 5.1 Overlaid contour plots

High MRR and low  $R_a$  are the two major attributes of EDM machining process. These two responses are conflicting in nature and hence achieving the both simultaneously by a set of optimum variables combination is difficult. In this section the multi response optimization is conceded out so that two conflicting goals are fulfilled concurrently. We resort to overlay contour plots which are comparatively simple approach to review the levels of operating parameters that satisfy two constrained objectives. It is considered that  $R_a$  in the range of  $1.067 \mu\text{m}$  to  $5 \mu\text{m}$  found to be reasonably good and acceptable for most of the applications. MRR has been set between a lower bound of  $0.1 \text{ mm}^3/\text{min}$  and upper bound of  $2.0 \text{ mm}^3/\text{min}$ . Thus constrained equation become:

$$1.067 < R_a < 5.0 \quad (10)$$

$$0.1 < \text{MRR} < 2.0 \quad (11)$$

The overlaid contour plots of MRR and  $R_a$  is shown in Fig. 5.

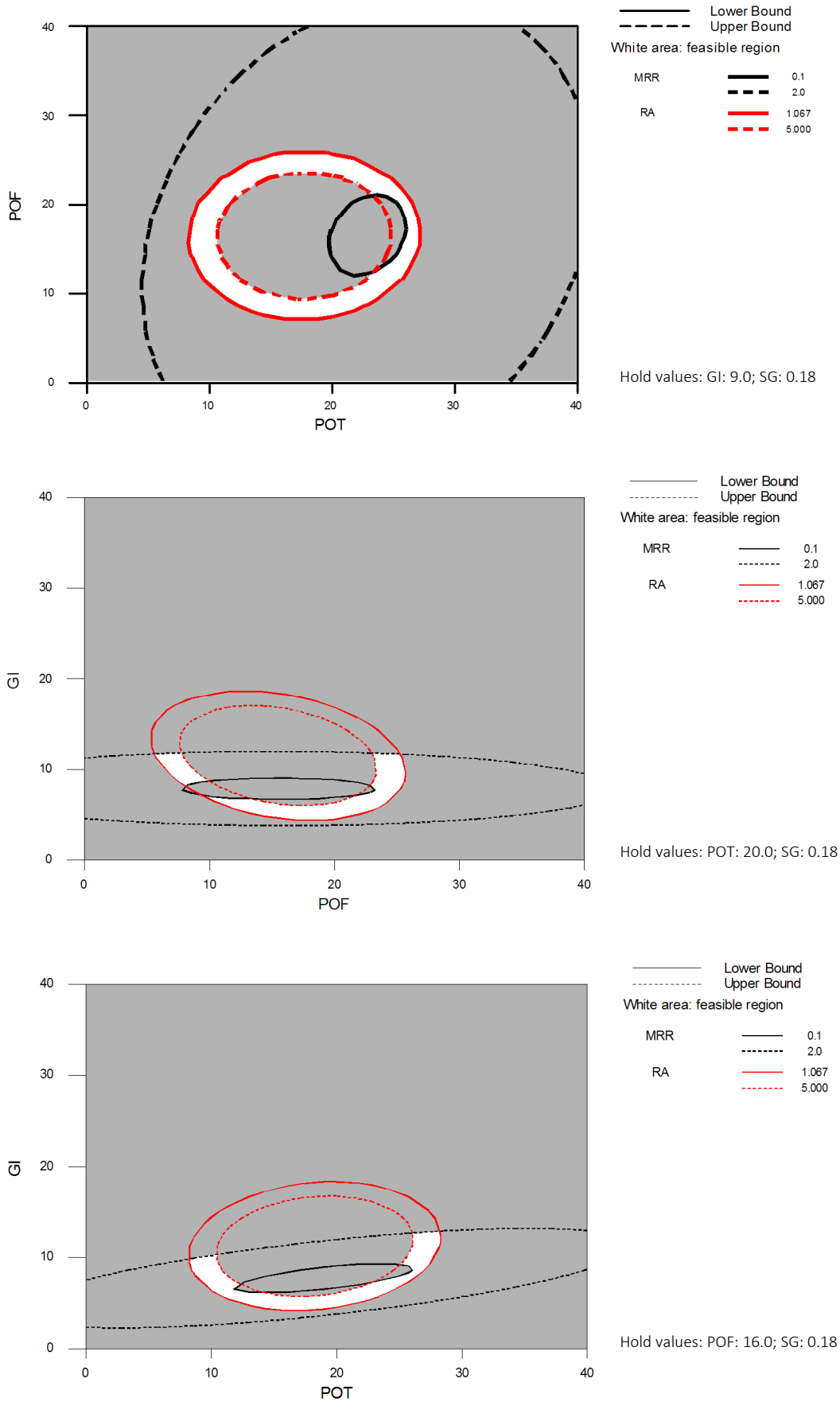


Fig. 5 Overlaid contour plot for MRR and  $R_a$

The overlaid contour plot of MRR and  $R_a$  with respect to POT, POF, and GI are portrayed. The bounded white areas (unshaded) as indicated in the figure are the region that simultaneously satisfies global objectives along with possible combinations of process variables. The plots advocate that combination of moderate POT and medium POF help achieve the targets. Corresponding value of GI and POF can be predicted from the curve with the hold value of POT and SG. The white area in the figure highlights for optimum MRR and  $R_a$  and corresponding value of GI and POT can be predicted from the curve with the hold value of POF and SG.

### 5.2 Desirability functions

Response optimizer helps to help recognize the factor settings that optimize a single response or a set of responses. For multiple responses, the necessities for all the responses in the set must be fulfilled. Response optimization is frequently helpful in product development when it is required to establish operating conditions that will effect in a product with desirable properties. Here the goal, lower, target, upper, and weight characterize the desirability function for each individual response. The importance (Import) parameters decide how the desirability functions are combined into a single composite desirability. The response optimization is shown in Table 6.

From the S/N ratio plot of Taguchi design we get highest MRR at combination of POT (16  $\mu$ s), POF (12  $\mu$ s), GI (11 A), SG (0.16 mm) and lowest  $R_a$  at combination of POT (24  $\mu$ s), POF (16  $\mu$ s), GI (7 A), SG (0.2 mm). Hence an optimized combination of POT (20  $\mu$ s), POF (16  $\mu$ s), GI (9 A), SG (0.18 mm) can be taken as starting point.

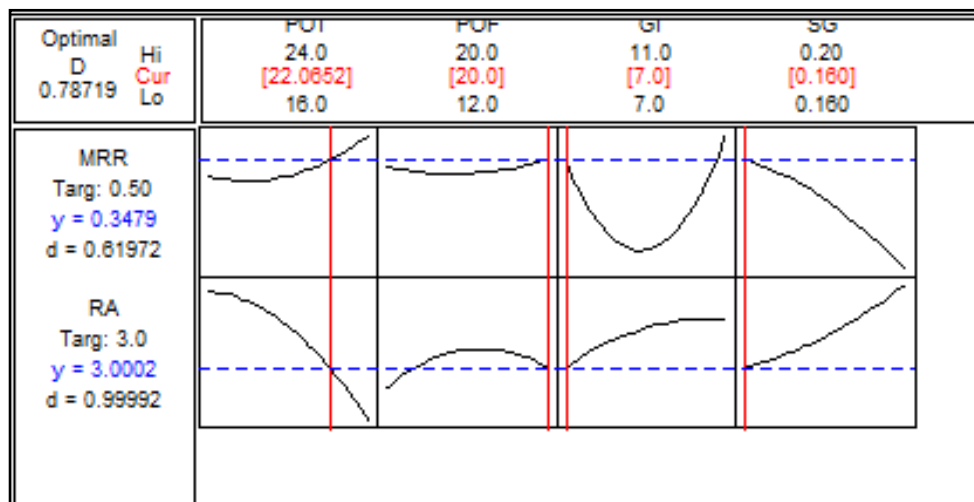
**Table 6** Desirability function results

Parameters	Goal	Lower	Target	Upper	Weight	Import
MRR	Maximum	0.100	0.5	2	1	1
$R_a$	Minimum	1.067	3.0	5	1	1

Predicted responses	Global solution
MRR = 0.34789, desirability is 0.61972 (61.972 %)	POT = 22.0652
$R_a$ = 3.00017, desirability is 0.99992 (99.9992 %)	POF = 20.0000
<b>Composite desirability is 0.78719 (78.719 %)</b>	GI = 7.0000
	SG = 0.1600

Fig. 6 represents the optimization plot of the responses (MRR and  $R_a$ ) with the process variables. It shows how the factors affect the predicted responses and allows to modify the factor settings interactively.



**Fig. 6** Plot showing responses (MRR and  $R_a$ ) against process variables

The figure shows the goal for the response, the predicted response,  $y$ , at the current factor settings, and the individual desirability score. The composite desirability,  $D$ , is displayed in the upper left corner of the graph. The label above the composite desirability refers to the current setting. When the optimization plot is created, the label is optimal. The vertical red lines on the graph represent the current factor settings. The horizontal dotted blue lines represent the current response values. From the earlier limit of MRR and  $R_a$  and assigning unbiased weight to the dual responses, the desirability of MRR becomes 0.91672 having predicted response of 0.34892 mm<sup>3</sup>/min. The same for  $R_a$  is  $d_{Ra} = 0.99992$  with the predicted response of 3.00017  $\mu$ m. Finally the dual desirability is 0.78719 having POT = 2.0652, POF = 20.0000, GI = 7.0000, SG = 0.1600 is the near optimal combination.

## 6. Discussion and conclusion

The experimental study indicates that in while machining AISI H13 tool steel using die sinking EDM process the responses are dependent on pulse on time, pulse off time, gap current and spark gap. The S/N ratio analysis along with ANOVA is a simple method to ascertain implication of several input parameters that administers multiple responses of the process. For higher MRR, GI is the most significant parameter and having contribution of 82.28 %. MRR increases with respect to increase of GI. In case of lower  $R_a$ , the POT is having the most significant effect and contributes 47.24 %.  $R_a$  decreases with the increase of POT and however  $R_a$  increases with increase of GI. For smaller overcut, SG is the most significant parameter and contributed 65.6 % and OC decreases with the increase of SG initially up to 0.18 mm then it increases with respect to SG.

The present work is carried out with a view to optimize MRR (maximize) and  $R_a$  (minimize) concurrently by employing a near optimal set of process variables. Since the optimization is carried out for a single pass machining, the due importance is given to the surface finish considering quality characteristics in a cost effective manner (enhanced productivity harnessing high MRR). This optimization is carried out by RSM that is promised to offer near optimal solution with little effort. The regression models are found to be worthy to express input-output relationship with a very high degree of predictability. The inferences drawn from the regression analysis is accentuated with the desirability functions. Gap current is found to be the most significant in comparison to the responses. The near optimal combinations of process variables are high POT, POF and low GI and SG to satisfy both the responses (MRR and  $R_a$ ) simultaneously. This set of inputs can be used to further optimize other functions like machining cost and can form the backbone of adaptive control strategies (adaptive control with optimization and geometric adaptive control). The overlaid contour plot is a good visual aid to identify the feasible region in regard to a set of input variables.

The individual desirability for each predicted responses are calculated. The individual desirability values are then combined into the composite desirability. The closer the predicted responses are to your target requirements, the closer the desirability will be to 1. The composite desirability combines the individual desirability into an overall value, and reflects the relative importance of the responses. The higher the desirability the closer it will be to 1. Here MRR has an intermediate desirability score of 0.61972 because the predicted response for MRR of 0.34789 is approximately two-thirds of the way between the target of 2 and the lower bound of 0.100. The goal for MRR was to maximize; therefore higher values are more desirable. Similarly  $R_a$  has a desirability score of 0.9999 because the predicted response of 3 is nearer to the target of 3. The experiment was less successful optimizing overcut than MRR and  $R_a$ , respectively. The composite desirability of 0.78719 places greater emphasis on MRR (importance is 2) than on  $R_a$  and overcut (importance is 1).

The RSM being a powerful tool, its potential can be extended to other areas of machining such as tool life, power and cutting force modeling. The experimental investigation for evaluating the optimal parametric combination and the subsequent effect of the parameters over the responses can act as an efficient and useful guideline for machining and manufacturing various metallic products.

The future work in this emerging area can be considered with other parameters and different responses such as cutting force, tool life etc. to capture the process in full perspective. The estimation of the reduction of the cost using multi-response optimized EDM process with respect to non-optimized die sinking EDM process can be further investigated. The average cost of energy consumption vs. cost of electrode material (and cost for electrode manufacturing) for the typical product manufactured by EDM process gives a scope for future work.

## References

- [1] Selvakumar, G., Sarkar, S., Mitra, S. (2013). An experimental analysis of single pass cutting of aluminium 5083 alloy in different corner angles through WEDM, *International Journal of Machining and Machinability of Materials*, Vol. 13, No. 2/3, 262-275, doi: [10.1504/IJMMM.2013.053227](https://doi.org/10.1504/IJMMM.2013.053227).
- [2] Kapoor, J., Khamba, J.S., Singh, S. (2012). The effect of machining parameters on surface roughness and material removal rate with cryogenic treated wire in WEDM, *International Journal of Machining and Machinability of Materials*, Vol. 12, No. 1/2, 126-141, doi: [10.1504/IJMMM.2012.048562](https://doi.org/10.1504/IJMMM.2012.048562).
- [3] Dvivedi, A., Kumar, P., Singh, I. (2010). Effect of EDM process parameters on surface quality of Al 6063 SiC<sub>p</sub> metal matrix composite, *International Journal of Materials and Product Technology*, Vol. 39, No. 3/4, 357-377.
- [4] Aligiri, E., Yeo, S.H., Tan, P.C., Zarepour, H. (2010). Benefits of using real-time pulse discriminating system in micro-EDM monitoring and control system, *International Journal of Mechatronics and Manufacturing Systems*, Vol. 3, No. 5/6, 466-481, doi: [10.1504/IJMMS.2010.036070](https://doi.org/10.1504/IJMMS.2010.036070).
- [5] Liu, H.S., Tarn, Y.S. (1997). Monitoring of the electrical discharge machining process by abductive networks, *The International Journal of Advanced Manufacturing Technology*, Vol. 13, No. 4, 264-270, doi: [10.1007/BF01179608](https://doi.org/10.1007/BF01179608).
- [6] Ayesta, I., Izquierdo, B., Sánchez, J.A., Ramos, J.M., Plaza, S., Pombo, I., Ortega, N., Bravo, H., Fradejas, R., Zamakona, I. (2013). Influence of EDM parameters on slot machining in C1023 aeronautical alloy, In: Lauwers, B., Kruth, J.-P. (eds.), *Procedia CIRP, Proceedings of the Seventeenth CIRP Conference on Electro Physical and Chemical Machining (ISEM)*, Vol. 6, Elsevier, 129-134, doi: [10.1016/j.procir.2013.03.059](https://doi.org/10.1016/j.procir.2013.03.059).
- [7] Nipanikar, S.R. (2012). Parameter optimization of electro discharge machining of AISI D3 steel material by using Taguchi method, *Journal of Engineering Research and Studies*, Vol. 3, No. 3, 7-10.
- [8] Ben Salem, S., Tebni, W., Bayraktar, E. (2011). Prediction of surface roughness by experimental design methodology in electrical discharge machining (EDM), *Journal of Achievements in Materials and Manufacturing Engineering*, Vol. 49, No. 2, 150-157.
- [9] Singh, K., Kalra, C.S. (2013). An experimental investigation: machining of OHNS steel by EDM, *Journal of Engineering Computers and Applied Sciences*, Vol. 2, No. 6, 39-42.
- [10] Syed, K.H., Palaniyandi, K., (2012). Performance of electrical discharge machining using aluminium powder suspended distilled water, *Turkish Journal of Engineering and Environmental Science*, Vol. 36, 195-207, doi: [10.3906/muh-1202-2](https://doi.org/10.3906/muh-1202-2).
- [11] Kumar, A., Kumar, V., Kumar, J. (2012). Prediction of surface roughness in wire electric discharge machining (WEDM) process based on response surface methodology, *International Journal of Engineering and Technology*, Vol. 2, No. 4, 708-719.
- [12] Kohli, A., Wadhwa, A., Virmani, T., Jain, U. (2012). Optimization of material removal rate in electrical discharge machining using fuzzy logic, *World Academy of Science, Engineering and Technology*, Vol. 6, No. 12, 1509-1514.
- [13] Mohanty, C.P., Sahu, J., Mahapatra, S.S. (2013). Thermal-structural analysis of electrical discharge machining process, In: Mehta, U. (ed.), *Procedia Engineering, Chemical, Civil and Mechanical Engineering Tracks of 3<sup>rd</sup> Nirma University International Conference on Engineering*, Vol. 51, 508-513, doi: [10.1016/j.proeng.2013.01.072](https://doi.org/10.1016/j.proeng.2013.01.072).
- [14] Arikatla, S.P., Krishnaiah, A., Mannan, K.T. (2013). Optimization of electric discharge machining response variables using design of experiments, *International Journal of Mechanical and Production Engineering*, Vol. 2 No. 1, 82-87.
- [15] Baseri, H., Aliakbari, E., Alinejad, G. (2012). Investigation of the rotary EDM process of X210Cr12, *International Journal of Machining and Machinability of Materials*, Vol. 11, No. 3, 297-307.
- [16] Park, S.H. (1996). *Robust design and analysis for quality engineering*, Chapman and Hall, London.
- [17] Montgomery, D.C. (2000). *Design and analysis of experiments*, Fifth edition, John Wiley & Sons, New York.